



LAWRENCE  
LIVERMORE  
NATIONAL  
LABORATORY

# Droplet-Based Segregation and Extraction of Concentrated Samples

C. R. Buie, P. Buckley, J. Hamilton, K. D. Ness, K. A. Rose

February 28, 2007

NSTI Nanotech 2007  
Santa Clara, CA, United States  
May 20, 2007 through May 24, 2007

## **Disclaimer**

---

This document was prepared as an account of work sponsored by an agency of the United States Government. Neither the United States Government nor the University of California nor any of their employees, makes any warranty, express or implied, or assumes any legal liability or responsibility for the accuracy, completeness, or usefulness of any information, apparatus, product, or process disclosed, or represents that its use would not infringe privately owned rights. Reference herein to any specific commercial product, process, or service by trade name, trademark, manufacturer, or otherwise, does not necessarily constitute or imply its endorsement, recommendation, or favoring by the United States Government or the University of California. The views and opinions of authors expressed herein do not necessarily state or reflect those of the United States Government or the University of California, and shall not be used for advertising or product endorsement purposes.

# Droplet-Based Segregation and Extraction of Concentrated Samples

C.R. Buie,<sup>1</sup> P. Buckley,<sup>2</sup> J. Hamilton,<sup>2</sup> K.D. Ness,<sup>2</sup> K.A. Rose<sup>2\*</sup>

<sup>1</sup>Department of Mechanical Engineering, Stanford University, Stanford, CA, USA

<sup>2</sup>Lawrence Livermore National Laboratory, Livermore, CA, USA

\*7000 East Avenue, L-223, Livermore, CA 94550, rose38@llnl.gov

## ABSTRACT

Microfluidic analysis often requires sample concentration and separation techniques to isolate and detect analytes of interest. Complex or scarce samples may also require an orthogonal separation and detection method or off-chip analysis to confirm results. To perform these additional steps, the concentrated sample plug must be extracted from the primary microfluidic channel with minimal sample loss and dilution. We investigated two extraction techniques; injection of immiscible fluid droplets into the sample stream (“capping”) and injection of the sample into an immiscible fluid stream (“extraction”). From our results we conclude that capping is the more effective partitioning technique. Furthermore, this functionality enables additional off-chip post-processing procedures such as DNA/RNA microarray analysis, real-time polymerase chain reaction (RT-PCR), and culture growth to validate chip performance.

## 1 INTRODUCTION

Incorporating microfluidic-based technologies into bio-analytical instruments has many benefits including reduced sample consumption, faster response times, and improved sensitivity. To achieve these benefits, microfluidic analysis often requires sample concentration and separation techniques, e.g., isotachopheresis (ITP), field amplified sample stacking (FASS), or electrophoretic separation, to improve the signal to noise ratio and identify analytes of interest. In some situations complex or scarce samples may also require an orthogonal separation and detection method, such as mass spectrometry or gel chromatography, for confirmation of results. To perform these additional steps, the concentrated sample plug must be extracted from the primary microfluidic channel with minimal sample loss and minimal dilution.

Several research groups are currently working on this issue. Lin et al. [1] demonstrated extraction of concentrated samples through constant control of complex electrode structures. They placed electrodes in strategic locations within microfluidic channels to manipulate charged samples. Similarly, Shaikh and Ugaz [2] used addressable electrode arrays to capture and manipulate DNA in a glass channel integrated with a silicon electrode and a printed circuit board. Lehmann et al. [3] have recently demonstrated the use of magnetic particles to manipulate microdroplets.

Here we explore sample extraction utilizing simple droplet and bubble generation techniques with precise metering and control of nanoliter scale fluid volumes. We investigated two techniques; injection of immiscible fluid droplets into the sample stream (“capping”) and injection of the sample into an immiscible fluid stream (“extraction”).

**Keywords:** sample manipulation, two phase, microfluidics, droplet

## 2 THEORY

In general, the key parameter in droplet creation dynamics is the capillary number defined as  $Ca = \mu u / \gamma$ , where  $\mu$  is the carrier fluid viscosity,  $u$  is the average velocity of the carrier fluid, and  $\gamma$  is the interfacial tension between the carrier and dispersed fluid. The capillary number represents the relative ratio of shear forces to surface tension forces on a growing droplet. For the experiments conducted in this study the capillary number is generally  $10^{-2}$  or lower, such that surface tension effects dominate. At low  $Ca$  the droplet formation follows a simple scaling law,

$$\frac{L}{w} = 1 + \frac{\alpha Q_{in}}{Q_{out}} \quad [1]$$

where  $L$  is length of the droplet,  $w$  is channel width,  $Q_{in}$  is the dispersed fluid flow rate,  $Q_{out}$  is the carrier fluid flow rate, and  $\alpha$  is a geometry dependent constant (usually of order one) [4]. When the microfluidic channel geometry is designed properly the length of the droplets created is a function of the immiscible fluid flow rate.

In the sample extraction technique the key parameter is  $L$ , the length of the droplet. In sample extraction the volume of sample extracted is directly proportional to the length of the sample droplet created (i.e. smaller  $L$  indicates smaller volume). Therefore, the amount of sample that can be manipulated is set by Equation [1]. Alternatively, the key parameter for sample capping is the spacing between droplets. During sample capping the spacing between immiscible droplets determines the volume of sample that can be manipulated. Equation [1] is not useful in determining the volume of sample that can be capped but we assume that this volume is proportional to  $Q_{out}/Q_{in}$  (higher carrier velocity yields larger droplet spacing and

larger capped fluid volume). Future work will include experimental determination of an appropriate droplet spacing relationship to predict capped fluid volume.

This work provides initial results to enable robust chip designs for high throughput sample analysis. We identify three figures of merit to help evaluate the designs. The figures of merit are >80% yield of original sample (volume extracted/segregated divided by initial sample volume), < 2X dilution of initial concentration, and completion of the extraction step within 5 s.

### 3 EXPERIMENTAL

#### 3.1 Microchip Fabrication

The microfluidic chips used in this study were fabricated using standard microfabrication techniques. The 40  $\mu\text{m}$  deep fluidic channels were etched in borosilicate glass with 1:1 hydrofluoric acid. Borosilicate glass was selected for compatibility with future sample pre-concentration and separation techniques.

Due to the hydrophilic nature of native glass, we used a surface coating to increase the contact angle in the microchannels. Hydrophobicity is critical to the creation of distinct sample regions since it prevents wicking of aqueous solution along the microchannel walls and in corners. Figure 1 shows a representative sample image of our glass microchannel without (a) and with (b) the hydrophobic treatment.

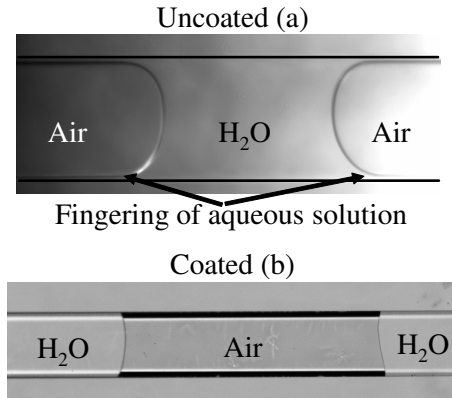


Figure 1: 200  $\mu\text{m}$  wide glass microchannels, untreated (a) and treated (b) with Tridecafluoro-1,1,2,2-tetrahydroctyl (TDFTS) for hydrophobicity.

#### 3.2 Experimental Setup

The experimental setup consists of an Olympus BX-61 microscope, and a Photometrics CoolSnap HQ charge coupled device camera with Uniblitz shutter for obtaining images. In addition, the setup features Valco multiposition valves and Harvard Apparatus PHD 2000 syringe pumps

for precise metering of fluid volumes. The entire setup is controlled via custom virtual instruments developed in LabView 7.

In Section 4.2 we discuss micron resolution particle image velocimetry [5, 6] measurements we made in our microchannels to validate numerical simulations. These measurements were taken with 1  $\mu\text{m}$  fluorescent beads (Molecular Probes, Eugene, OR) and a Pulnix TM 1040 video camera at 30 fps. Image analysis was performed using a published  $\mu\text{PIV}$  interrogation code. For a more thorough explanation of  $\mu\text{PIV}$  the reader is referred to refs. [5-7].

### 4 RESULTS

#### 4.1 Sample Capping

We first explored capping of samples with immiscible fluids such as air and Fluorinert<sup>TM</sup> FC-77 (3M<sup>TM</sup>) using a T-channel droplet injector similar to the injectors used by other research groups [8-10]. Figure 2 depicts fluorescent samples (1 mM Fluorescein in water) capped with Fluorinert. These samples exhibited no diffusion or detectable loss in concentration over thirty minutes. Our experimental study indicated that capping with incompressible Fluorinert droplets provided more reproducible results compared to air. Due to the compressibility of air, it was exceedingly difficult to control the nanoliter scale volumes necessary to cap the sample.

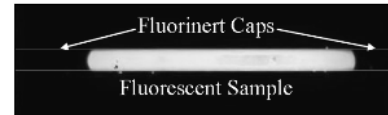


Figure 2. Demonstration of sample capping technique in which Fluorinert droplets are injected around a sample.

This technique segregates the sample and enables extraction with minimal loss and dilution.

#### 4.2 Sample Extraction

The sample segregation, or extraction technique was explored with a combination of experimental and computational studies conducted in COMSOL Multiphysics. First we conducted  $\mu\text{PIV}$  experiments in our 240  $\mu\text{m}$  wide glass channels with T-junctions. These results were compared with our computational results for fluid flow in the channel. Figure 3 shows measured (a) and simulated (b) velocity fields when the fluid flow is from east to south. The figures present qualitative evidence that our COMSOL model correctly accounts for the relevant flow physics in the channel.

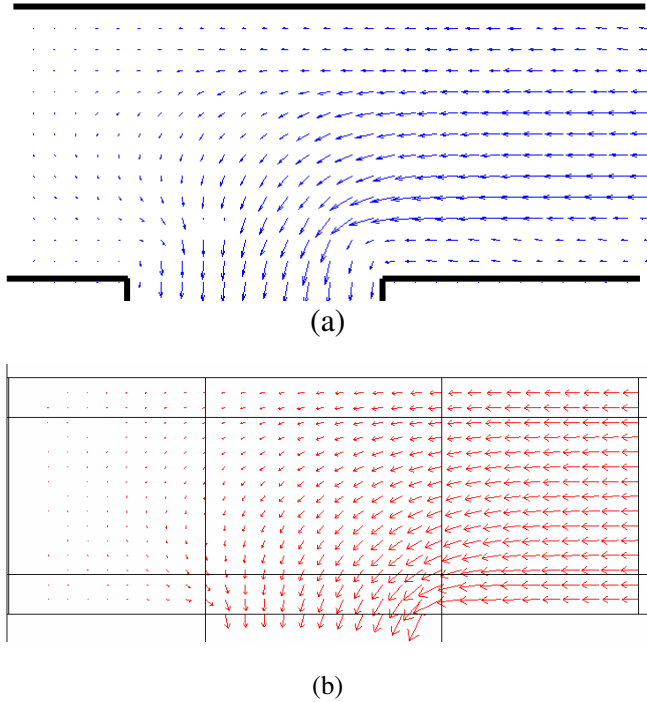


Figure 3:  $\mu$ PIV experiment (a) and COMSOL simulation (b) for pressure driven flow from east to south at the T-junction of a 240  $\mu\text{m}$  wide, 40  $\mu\text{m}$  deep channel.

### 4.3 Simulations of Sample Extraction

In addition to  $\mu$ PIV, we performed numerical simulations of sample extraction using a T-channel similar to those shown in Figure 3. The purpose of this section is to evaluate potential chip designs and extraction schemes before fabricating chips. Here we assume that prior to the sample extraction step the sample has been concentrated into a Gaussian shaped sample plug. This assumption is directly applicable to potential applications for these chips in which the sample extraction occurs directly after a pre-concentration step such as temperature gradient focusing or isotachopheresis. Once again we assume 240  $\mu\text{m}$  wide, 40  $\mu\text{m}$  deep carrier channels but we use two different extraction channel widths (45  $\mu\text{m}$  and 240  $\mu\text{m}$ ). The simulated flow rate in both cases is 50  $\mu\text{l}/\text{min}$  and the simulated solute is rhodamine with a diffusivity of  $2.48 \times 10^{-10} \text{ m}^2/\text{s}$ . Since one of our figures of merit is to extract samples within 5 s, we used this as the simulation time for both cases. Note that the flow in this case is from west to north.

As can be seen from Figure 4 there is some qualitative difference between the 45  $\mu\text{m}$  and 240  $\mu\text{m}$  side channels. At the end of the simulation (after 5 s), most of the sample can still be seen in the 240  $\mu\text{m}$  side channel while nearly all of the sample that makes it into the 45  $\mu\text{m}$  side channel has advected away. The reason for this is the significantly higher average channel velocity in the 45  $\mu\text{m}$  channel case due to its smaller cross sectional area. The average

velocity is more than 5 times higher in the smaller channel so the residence time of the simulated rhodamine is shorter.

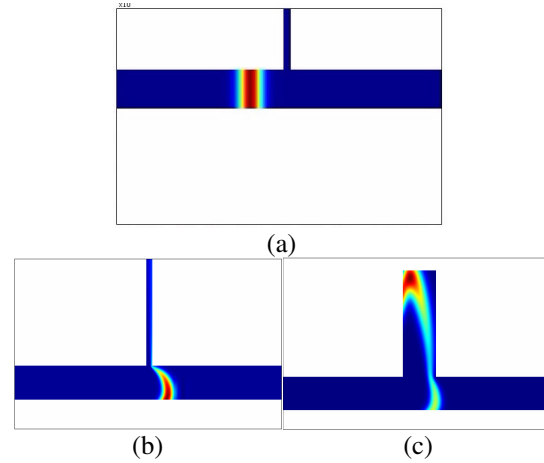


Figure 4: Initial rhodamine concentration profile (a) and final (after 5 s) concentration profile for the 45  $\mu\text{m}$  and 240  $\mu\text{m}$  (c) side channels.

Quantitative measurements of sample dilution and percentage of sample extracted are given in Figure 5. As can be expected, the amount/percentage of sample extracted increases with time but begins to flatten after roughly 5 s. The percentage of sample extracted does not flatten out at 100% due to the effects of the velocity profile in the channel and diffusion. Some of the simulated rhodamine is advected past the extraction channel where its transport becomes diffusion limited. In this region the solute is free to diffuse in any direction and can slowly move away from the extraction channel. We found that in both cases (240  $\mu\text{m}$  and 45  $\mu\text{m}$  side channels) the dilution of the sample and amount extracted were similar. See Table I for a brief summary.

Table I: Extraction Statistics

| Side Channel      | % Dilution | % Extracted (after 5s) |
|-------------------|------------|------------------------|
| 45 $\mu\text{m}$  | 14.8%      | 86.2%                  |
| 240 $\mu\text{m}$ | 13.3%      | 84.4%                  |

## 5 SUMMARY AND FUTURE WORK

We have presented preliminary sample extraction techniques for microfluidic chips. We demonstrated how numerical modeling and  $\mu$ PIV can aid in chip design and showed preliminary sample extraction simulations. Based on the significant dilution (Table I) in the sample extraction technique, we conclude that sample capping, as shown in Figure 2 is a better technique and holds more potential to achieve our figures of merit. In the future we will integrate this technique with other on-chip pre-concentration and analysis tools in order to move closer to a micro total analysis system.

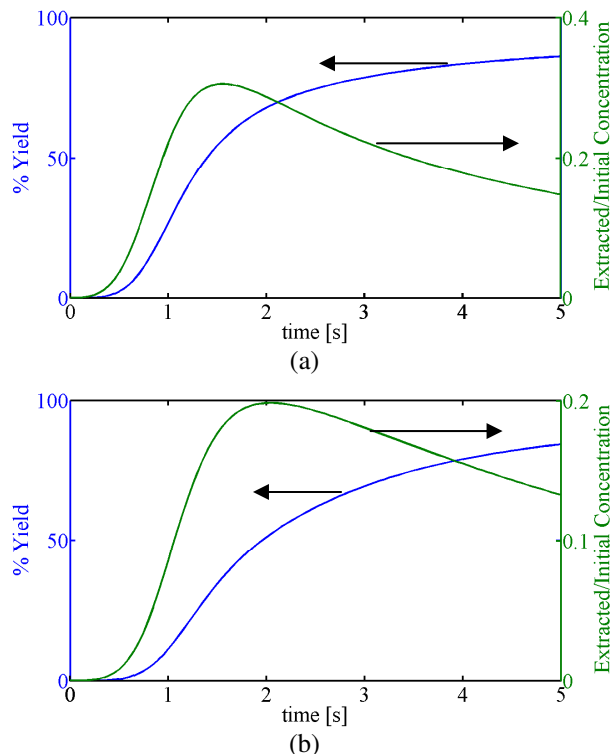


Figure 5: % Yield and sample dilution for the 45  $\mu\text{m}$  (a) and 240  $\mu\text{m}$  (b) side channels.

## REFERENCES

1. R. Lin, D.T. Burke, M.A. Burns, *Analytical Chemistry*, 77 (2005) 4338-4347.
2. F.A. Shaikh, V.M. Ugaz, *Proceedings of the National Academy of Sciences of the United States of America*, 103 (2006) 4825-30.
3. D. Kramer, J.B. Zhang, R. Shimo, E. Lehmann, A. Wokaun, K. Shinohara, G.G. Scherer, *Electrochimica Acta*, 50 (2005) 2603-2614.
4. P. Garstecki, M.J. Fuerstman, M.A. Fischbach, S.K. Sia, G.M. Whitesides, *Lab on a Chip*, 6 (2006) 207-212.
5. C.D. Meinhart, S.T. Wereley, J.G. Santiago, *Journal of Fluids Engineering-Transactions of the Asme* ;, 122 (2000) 285-289.
6. J.G. Santiago, S.T. Wereley, C.D. Meinhart, D.J. Beebe, R.J. Adrian, *Experiments in Fluids* ;, 25 (1998) 316-319.
7. C.D. Meinhart, S.T. Wereley, J.G. Santiago, *Experiments in Fluids* ;, 27 (1999) 414-419.
8. L.-H. Hung, K.M. Choi, W.-Y. Tseng, Y.-C. Tan, K.J. Shea, A.P. Lee, *Lab on a Chip*, 6 (2006) 174-178.
9. Y.-C. Tan, V. Christini, A.P. Lee, *Sensors and Actuators B*, 114 (2006) 350-356.
10. P. Gartecki, M.J. Fuerstman, H.A. Stone, G.M. Whitesides, *Lab on a Chip*, 6 (2006) 437-446.

This work was performed under the auspices of the U. S. Department of Energy by University of California, Lawrence Livermore National Laboratory under contract W-7405-Eng-48.